Membrane Biology:

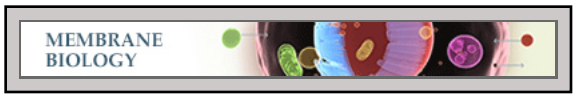

Syntaxin 16 Binds to Cystic Fibrosis Transmembrane Conductance Regulator and Regulates Its Membrane Trafficking in Epithelial Cells

Heon Yung Gee, Bor Luen Tang, Kyung Hwan Kim and Min Goo Lee

J. Biol. Chem. 2010, 285:35519-35527.
doi: 10.1074/jbc.M110.162438 originally published online September 8, 2010

THE JOURNAL OF BIOLOGICAL CHEMISTRY VOL. 285, NO. 46, pp. 35519–35527, November 12, 2010

Syntaxin 16 Binds to Cystic Fibrosis Transmembrane Conductance Regulator and Regulates Its Membrane Trafficking in Epithelial Cells*[S]

Received for publication, July 8, 2010, and in revised form, September 1, 2010 Published, JBC Papers in Press, September 8, 2010, DOI 10.1074/jbc.M110.162438

Heon Yung Gee[‡], Bor Luen Tang[§], Kyung Hwan Kim[‡], and Min Goo Lee[‡1]

From the [‡]Department of Pharmacology, Institute of Gastroenterology, and Brain Korea 21 Project for Medical Sciences, Yonsei University College of Medicine, Seoul 120-752, Korea and the [§]Department of Biochemistry, Yong Loo Lin School of Medicine, National University of Singapore, 117597, Singapore

The cystic fibrosis transmembrane conductance regulator (CFTR) is a key membrane protein in the complex network of epithelial ion transporters regulating epithelial permeability. Syntaxins are one of the major determinants in the intracellular trafficking and membrane targeting of secretory proteins. In the present study we demonstrate the biochemical and functional association between CFTR and syntaxin 16 (STX16) that mediates vesicle transport within the early/late endosomes and trans-Golgi network. Immunoprecipitation experiments in rat colon and T84 human colonic epithelial cells indicate that STX16 associates with CFTR. Further analyses using the domain-specific pulldown assay reveal that the helix domain of STX16 directly interacts with the N-terminal region of CFTR. Immunostainings in rat colon and T84 cells show that CFTR and STX16 highly co-localize at the apical and subapical regions of epithelial cells. Interestingly, CFTR-associated chloride current was reduced by the knockdown of STX16 expression in T84 cells. Surface biotinylation and recycling assays indicate that the reduction in CFTR chloride current is due to decreased CFTR expression on the plasma membrane. These results suggest that STX16 mediates recycling of CFTR and constitutes an important component of CFTR trafficking machinery in intestinal epithelial cells.

The cystic fibrosis transmembrane conductance regulator (CFTR)[2] is an ion channel that transports chloride ions (Cl^-). CFTR plays an important role in the secretion and absorption of ions and fluid across the luminal surface in diverse epithelia (1). Cystic fibrosis (CF), the most common genetic disease with pubescent lethality in Caucasians, is caused by CFTR gene mutations. Among more than 1400 genetic variations identified to date, loss of the phenylalanine residue at position 508 (ΔF508-CFTR) is the most prevalent disease-causing mutation and is carried by 90% of CF patients (2). The ΔF508-CFTR exhibits a trafficking defect that prevents its exit from the endoplasmic reticulum (ER) and is eventually targeted for degradation via ER quality control machinery. However, ΔF508-CFTR is known to harbor some degree of chloride channel activity once it reaches the cell surface (2). Characterizing factors involved in CFTR intracellular trafficking will help elucidate CF pathophysiology and provide therapeutic targets to modulate the biosynthetic pathway of CFTR.

The elements involved in vesicle trafficking and the delivery of CFTR have been partially identified. Small GTPases, including Sar1, Arf1, and Rab proteins affect the processing and trafficking of CFTR (3, 4). Several studies have also demonstrated a relationship between CFTR and proteins of the soluble *N*-ethylmaleimide-sensitive factor attachment protein receptor (SNARE) family, which mediates the fusion of intracellular vesicles with target membranes in eukaryotic cells. Among the SNARE family, syntaxins (STXs) belong to a subfamily of target (t)-SNAREs stationed at the target membrane. The SNARE domain of STX consists of an ~60-residue membrane-proximal coiled-coil domain and mediates membrane fusion through its interaction with SNARE domains of the cognate vesicle (v)-SNARE partners found on specific vesicle membranes (5). Recent studies have shown that STXs also interact with a wide range of proteins other than their cognate SNARE partners. For example, STX1A and STX3 interact with epithelial cell sodium channels, thereby regulating the intrinsic properties and cell-surface expression of these channels (6). Interestingly, several syntaxins, such as STX1A and STX13, are also known to be involved in CFTR trafficking and activity (4, 7), and current knowledge of STXs associated with CFTR regulation is listed in supplemental Table 1.

We found that STX16, an additional member of syntaxin that mediates vesicle transport within the early/late endosomes and trans-Golgi network (TGN) (5, 8), associates with CFTR in a preliminary screening. The present study aims to examine the regulation of CFTR via STX16 in the physiologically relevant conditions. The results in this study suggest that STX16 mediates the apical targeting and/or recycling of CFTR and constitutes an important component of the CFTR trafficking machinery in intestinal epithelial cells.

* This work was supported by National Research Foundation of Korea Grants 2007-0055732, 2010-0001670, and 2010-0017752 from the Ministry of Education, Science, and Technology, Korea.

[S] The on-line version of this article (available at http://www.jbc.org) contains supplemental Tables 1 and 2 and Figs. 1–3.

[1] To whom correspondence should be addressed: Dept. of Pharmacology, Yonsei College of Medicine, 134, Sinchon-Dong, Seodaemun-Gu, Seoul 120-752, Korea. Tel.: 82-2-2228-1737; Fax: 82-2-313-1894; E-mail: mlee@yuhs.ac.

[2] The abbreviations used are: CFTR, cystic fibrosis (CF) transmembrane conductance regulator; SNARE, soluble *N*-ethylmaleimide-sensitive factor attachment protein receptor; STX, syntaxin; NBD, nucleotide binding domain; ER, endoplasmic reticulum; TGN, trans-Golgi network; NMDG-Cl, *N*-methyl-D-glucamine chloride; pF, picofarads; aa, amino acids.

EXPERIMENTAL PROCEDURES

Plasmids, Cell Culture, and Transfection—The pCI-neo-myc-STX16 plasmid was previously described (9). The pCMV-CFTR plasmid (pCMVNot6.2) was a gift from Dr J. Rommens at the Hospital for Sick Children (Toronto, ON, Canada). The mammalian expressible hemagglutinin (HA)-tagged CFTR plasmids were constructed using a polymerase chain reaction (PCR)-based method. Briefly, cDNA encoding the full-length CFTR was PCR-amplified from pCMV-CFTR. A fragment containing CFTR was subcloned into a modified pcDNA3.1 (Invitrogen) using the XhoI and NotI restriction sites to construct a plasmid with an HA tag at the N terminus of CFTR (HAN-CFTR). The N terminus deleted variant of HAN-CFTR was made by inserting PCR fragment (aa 81-stop codon) into the HA-tagged pcDNA3.1 using the XhoI and NotI restriction sites. The CFTR construct with the HA tag at the second extracellular loop of CFTR (HA-CFTR) was made by inserting a sequence encoding the amino acids ASYDHSRNNYPYDVPDYASYAVIPDNK between Glu-217 and Leu-218 of CFTR according to the protocol described previously (3). The C terminus-deleted variants of HA-CFTR were made by generating stop codons at the designated sites using a PCR-based mutagenesis technique. Four glutathione *S*-transferase (GST) fusion domains of CFTR (N-term (aa 1–79), NBD1 (aa 433–584), NBD2 (aa 1219–1382), and C-term (aa 1387–1480)) were generated by inserting PCR fragments amplified from pCMV-CFTR into EcoRI/NotI sites of the bacterial expression vector pGEX-4T-1 (GE Healthcare). Four histidine His_6 fusion domains of STX16 were generated by inserting PCR fragments (N-term (aa 1–77), Habc (aa 78–239), SNARE (aa 234–302), ΔTM (aa 1–302)) into the bacterial expression vector pET-28c(+) (Novagen, Darmstadt, Germany) using EcoRI/NotI or EcoRI/XhoI sites.

HEK 293 cells were maintained in high glucose Dulbecco's modified Eagle's medium (DMEM-HG; Invitrogen) supplemented with 10% fetal bovine serum, penicillin (50 IU/ml), and streptomycin (50 μg/ml). Plasmids were transiently transfected into HEK 293 cells using Lipofectamine Plus Reagent (Invitrogen). T84 human colonic epithelia cells were maintained in a 1:1 mixture of Ham's F-12 medium and DMEM supplemented with 10% fetal bovine serum, penicillin (50 IU/ml), and streptomycin (50 μg/ml). The STX16-specific or control scrambled small interfering (si) RNAs were purchased from Qiagen (Valencia, CA). siRNAs or plasmids were transiently transfected into T84 cells using Lipofectamine 2000 (Invitrogen). Transfection efficiency of >90% for the siRNA treatment was confirmed in T84 cells using FITC-labeled siRNA and conventional epifluorescence microscopy.

Immunoblotting, Immunoprecipitation, and Immunocytochemistry—Immunoblotting and immunoprecipitation were performed as described previously (10). For immunoprecipitation, cell and tissue lysates were mixed with the appropriate antibodies and incubated overnight at 4 °C in a lysis buffer containing 50 mM Tris-HCl (pH 7.4), 200 mM NaCl, 1% (v/v) Nonidet P-40, 0.25% (v/v) sodium deoxycholate, and complete protease inhibitor mixture (Roche Applied Science). Immune complexes were collected by binding to mixed protein A/G beads and then washed four times with lysis buffer prior to electrophoresis. For immunoblotting, protein samples were suspended in a sodium dodecyl sulfate (SDS) buffer and separated by SDS-polyacrylamide gel electrophoresis. The separated proteins were transferred to a nitrocellulose membrane and blotted with appropriate primary and secondary antibodies. Protein bands were detected by enhanced chemiluminescence (Amersham Biosciences), and the staining intensities of immunoblots were analyzed using imaging software (Multi Gauge Version 3.0, Fujifilm, Valhalla, NY).

For immunocytochemistry, T84 cells were fixed and permeabilized by incubation in cold methanol for 10 min at −20 °C 3 days after transfection. Immunostaining of frozen sections was performed as described previously (11). Briefly, colon tissues from Sprague-Dawley rats were embedded in optimal cutting temperature (OCT) compound (Miles, Elkhart, IN), frozen in liquid nitrogen, and then cryosectioned into 4-μm sections. Nonspecific binding sites were blocked by incubation for 1 h at room temperature with 0.1 ml of phosphate-buffered saline (PBS) containing 5% goat serum, 1% bovine serum albumin, and 0.1% gelatin (blocking medium). After blocking, cells were stained by incubation with appropriate primary antibodies and then treated with fluorophore-tagged secondary antibodies. Image analyses were carried out using MetaMorph software (Molecular Devices, Sunnyvale, CA). Anti-STX16 was described previously (12), and anti-CFTR M3A7 (Millipore, Billerica, MA), anti-calnexin (Abcam, Cambridge, MA), anti-BiP (Cell Signaling, Inc., Danvers, MA), anti-β actin, anti-HA, anti-Myc, anti-His, and anti-Aldolase A (Santa Cruz Biotechnology, Santa Cruz, CA) antibodies were purchased from commercial sources. Rabbit polyclonal anti-CFTR antibody (R4) was raised against peptides corresponding to amino acids at 1458–1471 of human CFTR (CKSKPQIAALKEET) and affinity-purified.

Subcellular Fractionation—Subcellular fractionation was performed as described previously (13). Culture dishes (100 mm) of T84 cells were rinsed 3 times with 10 ml of HES buffer containing 255 mM sucrose, 20 mM HEPES (pH 7.4), and 1 mM EDTA. Cells were harvested in HES buffer (4 ml) containing complete protease inhibitor mixture and homogenized. The homogenate was centrifuged at 19,000 × *g* for 20 min. The resulting supernatant was centrifuged at 41,000 × *g* for 20 min to yield a high density microsome fraction pellet. Then the supernatant was further centrifuged at 180,000 × *g* for 75 min to yield a low density microsome pellet. The pellet obtained from the initial centrifugation step was layered onto 1.12 M sucrose in HES buffer and centrifuged at 100,000 × *g* in a Beckman SW-41 rotor for 60 min. This yielded a white fluffy band at the interface (plasma membrane fraction) and a viscous brown pellet (mitochondria/nuclei fraction). The plasma membrane fraction was resuspended in 1 ml of HES and pelleted at 40,000 × *g* for 20 min.

Surface Biotinylation—Surface biotinylation of CFTR was performed as described previously (10). T84 cells were grown on a permeable support (Corstar Transwell, Corning Life Sciences, NY) to form monolayers, and siRNAs were transfected at day 6. The siRNA transfection was repeated twice with 3-day intervals. Forty-eight hours after the second siRNA transfection, T84 cells were cooled to 4 °C and washed three times with

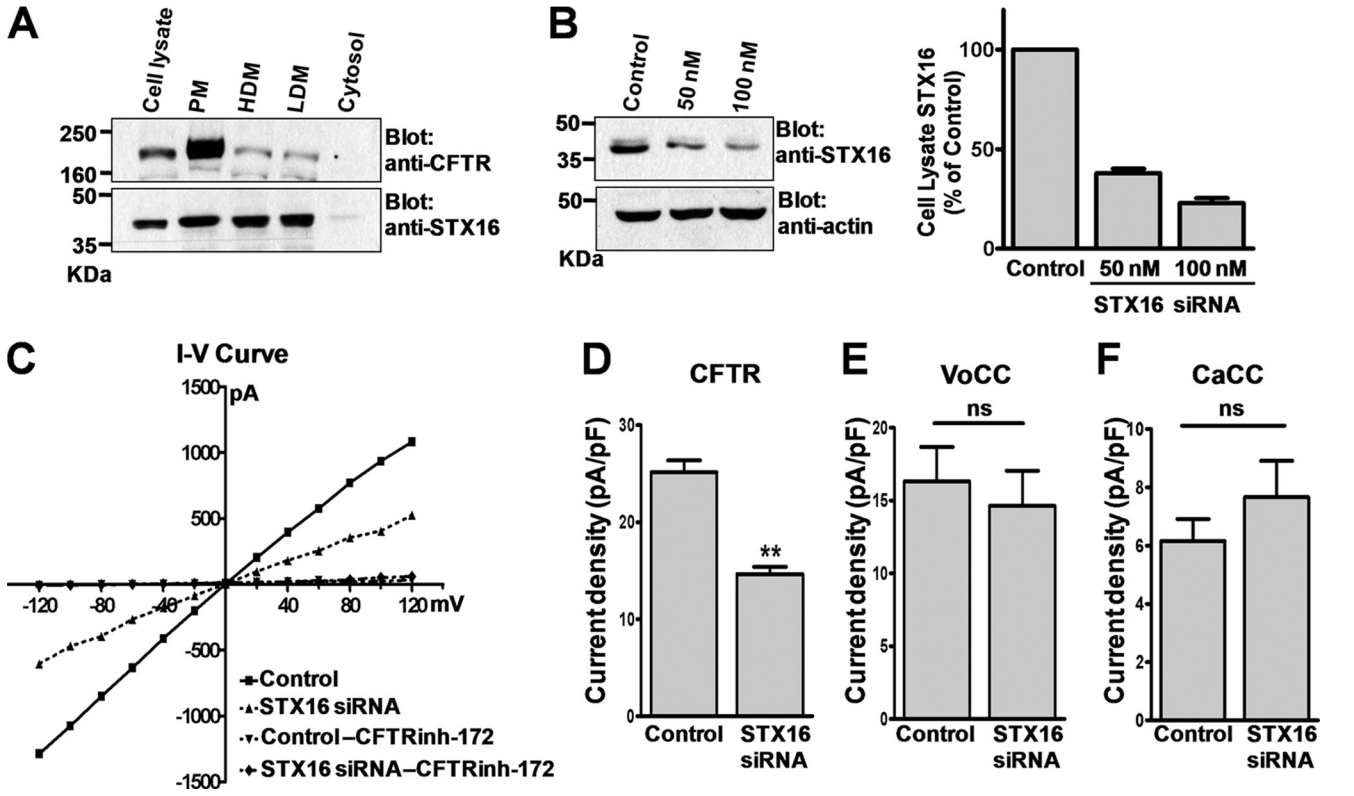

FIGURE 1. **Effect of STX16 depletion on CFTR current in T84 cells.** *A*, subcellular localization of STX16 in T84 cells is shown. Plasma membrane (*PM*), high density microsome (*HDM*), low density microsome (*LDM*), and cytosol fractions were prepared by differential centrifugation. Fractions were immunoblotted for CFTR and STX16. Each *lane* was loaded with 20 μg of protein except for CFTR cell lysate (100 μg). *B*, protein samples were obtained from T84 cells 48 h after transfection with the control scrambled (100 nM) or STX16-specific (50 or 100 nM) siRNA. Equal amounts of protein samples (20 μg) were immunoblotted with STX16 and β-actin antibodies. A summary of three separate experiments is presented in the *right panel*. *C*, the cAMP-activated Cl^- channel activity was measured in the whole-cell configuration. The current-voltage (*I-V*) relationships were obtained with a step pulse from -120 to $+120$ mV applied at peak current. T84 cells were pretreated with the control or STX16-specific siRNA (100 nM) for 48 h. Treatment with forskolin (5 μM), an adenylyl cyclase activator, evoked a Cl^- current that was sensitive to the CFTR inhibitor CFTRinh-172 (10 μM) in T84 cells. *D*, a summary of CFTR channel activity measurements is shown. Mean currents measured at -40 mV holding potential were normalized as current densities (pA/pF; cells transfected with control siRNA, $n = 14$; cells transfected with STX16 siRNA, $n = 11$). *E*, a summary of volume-sensitive Cl^- channel (*VoCC*) activity measurements is shown. The current was activated by reducing the osmolarity of the bath solution from 323 to 278 mosM (cells with control siRNA, $n = 10$; cells with STX16 siRNA, $n = 9$). *F*, a summary of Ca^{2+}-activated Cl^- channel (*CaCC*) activity measurements is shown. The current was activated by 400 nM free Ca^{2+} in pipette solution (cells with control siRNA, $n = 13$; cells with STX16 siRNA, $n = 14$). **, $p < 0.01$, difference from control; *ns*, not significant.

PBS. The plasma membrane proteins were then biotinylated by gently shaking the cells in PBS buffer containing sulfo-NHS-SS-biotin (Pierce) for 30 min. After biotinylation, cells were washed extensively with quenching buffer to remove excess biotin and then washed twice with PBS. The cells were lysed and incubated overnight at 4 °C with avidin solution (UltraLink Immobilized NeutrAvidin Beads 10%, Pierce). Avidin-bound complexes were pelleted by centrifugation at 13,000 rpm and washed 3 times. Biotinylated proteins were eluted in 2× sample buffer, resolved by SDS-PAGE, electrotransferred, and immunoblotted with anti-CFTR M3A7.

Apical Recycling Assay—Apical recycling of internalized CFTR was assayed in T84 cells as described previously (14). Because it is difficult to positively visualize the recycled CFTR, the amount of apically recycled CFTR was estimated by subtracting non-recycled CFTR from total internalized CFTR. Briefly, the plasma membrane proteins were biotinylated and then internalized for 30 min at 37 °C. Proteins remaining at the cell surface after 30 min were stripped of biotin with four 15-min washes in the sodium 2-mercaptoethanesulfonate stripping buffer (50 mM MESNA, 150 mM NaCl, 1 mM EDTA, 0.2% BSA, and 20 mM Tris (pH 8.6)). To detect the recycling of internalized, biotinylated CFTR, T84 cells were incubated at 37 °C and stimulated with 5 μM forskolin for 0, 5, 10, or 20 min and then quickly cooled to 4 °C. Biotinylated CFTR that is recycled to the plasma membrane was then stripped of biotin by the MESNA buffer washes. The remaining non-recycled biotinylated CFTR was detected as described above.

Pulldown Assays—The pulldown assay was performed as described previously (15). All recombinant fusion proteins were produced in BL-21 (DE3) *Escherichia coli* strain. Briefly, synthesis of GST fusion and His_6 fusion proteins was induced by 0.5 mM isopropyl β-D-1-thiogalactopyranoside at 30 °C. Recombinant proteins were subsequently purified with glutathione-Sepharose™ beads (Amersham Biosciences) or with a nickel-nitrilotriacetic acid protein purification system (Qiagen) according to the manufacturer's instructions. Eluted His_6 fusion proteins were mixed with 50 μg of GST fusion recombinant proteins bound to glutathione-Sepharose™. After overnight incubation at 4 °C, bead-bound complexes were washed, eluted in SDS sample buffer, and immunoblotted.

Measurement of Cl^- Channel Activities—Whole-cell recordings were performed on T84 cells as reported previously (16). Cl^- currents were isolated by using Cl^- as the only permeant

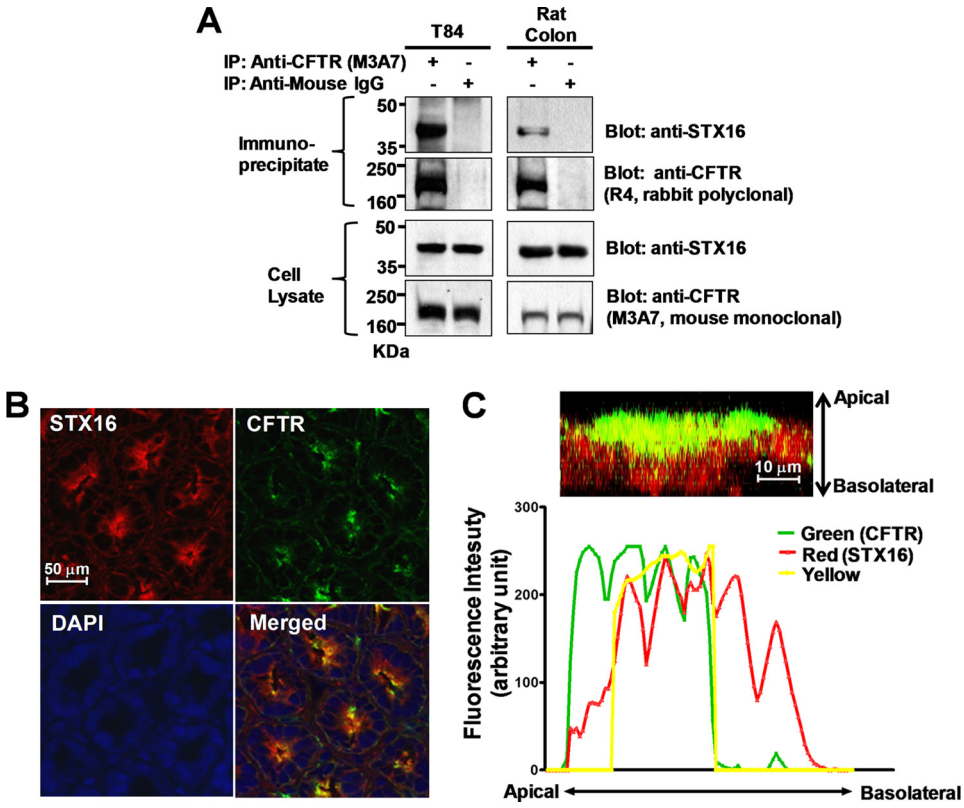

FIGURE 2. **CFTR and STX16 associate *in vivo*.** *A*, co-immunoprecipitation (*IP*) of STX16 and CFTR in T84 cell and rat colon is shown. Protein samples were precipitated with control (nonimmune IgG) and anti-CFTR M3A7. Immunoblotting was then carried out using anti-STX16. Co-immunoprecipitation was performed with a total of 1 mg lysate, and each lane in lysate blot was loaded with 60 μg of protein. *B*, rat colon slices were immunofluorescently stained with anti-STX16 (*red*) and anti-CFTR M3A7 (*green*). The nuclei were stained with 4′,6-diamidino-2-phenylindole (*DAPI*). *C*, localization of CFTR and STX16 in T84 monolayers is shown. Exogenous CFTR was additionally expressed using transient transfection with pCMV-CFTR. Fluorescent images of the vertical *z* axis section were obtained after staining with anti-STX16 (*red*) and anti-CFTR (*green*) using a Zeiss LSM 510 confocal microscope. Fluorescence intensities of the various emissions were analyzed with MetaMorph software.

densities (pA/pF). CFTRinh-172, a CFTR inhibitor was purchased from Sigma.

RESULTS

Depletion of STX16 Down-regulates CFTR Channel Activity—We first investigated STX16 distribution in T84 colonic epithelial cells, which endogenously express CFTR and STX16. Among the known splice variants of human STX16 (17), STX16A, 16B, and 16H isoforms harbor a single transmembrane domain, whereas STX16C and 16D isoforms are cytosolic proteins that lack the transmembrane domain. To determine the subcellular localization of STX16 in T84 cells, cellular compartments were fractionated by differential centrifugation (Fig. 1*A*). The high density microsome fraction contains large endosomal components and the ER, whereas the low density microsome fraction contains Golgi endosomes and small vesicles. Cellular fractionation followed by immunoblotting showed that CFTR was primarily observed in the plasma membrane fraction, and STX16 was detected in the plasma membrane, high density microsome, and low density microsome fractions but not in the cytosol. Therefore, STX16 is present largely in membrane-bound forms in T84 cells. Further identification by reverse transcription PCR using isoform-specific primers revealed that STX16A (isoform b in the National Center for Biotechnology Information data base, www.ncbi.nlm.nih.gov) is the major isoform expressed in T84 cells (supplemental Fig. 1 and supplemental Table 2).

We used a siRNA-mediated expression silencing approach to determine the role of STX16 on CFTR function in epithelial cells. Initially, the efficiency of siRNA directed against STX16 was assessed in T84 cells (Fig. 1*B*). STX16 expression was decreased by 77.2 ± 6.3% in cells transfected with STX16 siRNA (100 nM) compared with scrambled siRNA-treated cells. The effect of STX16 depletion on CFTR channel activity was measured with the whole-cell patch clamp technique (Fig. 1*C*). Treatment with forskolin, an adenylyl cyclase activator, evoked a large cAMP-stimulated CFTR-induced inward current that was sensitive to the CFTR inhibitor CFTRinh-172 (Fig. 1*C*). Notably, STX16 depletion induced a remarkable reduction in the CFTR Cl^- channel activity. The CFTR current density (pA/pF) was decreased by 42.6 ± 5.3% in STX16-depleted cells (Fig. 1*D*). However, STX16 knockdown had no significant effect on the volume-sensitive (*VoCC*) and Ca^{2+}-activated (*CaCC*) Cl^-

ion in the pipette and bath solutions. For CFTR currents, the pipette solution contained 140 mM *N*-methyl-D-glucamine chloride (NMDG-Cl), 5 mM EGTA, 1 mM $MgCl_2$, 1 mM Tris-ATP, and 10 mM HEPES (pH 7.4), and the bath solution contained 140 mM NMDG-Cl, 1 mM $CaCl_2$, 1 mM $MgCl_2$, 10 mM glucose, and 10 mM HEPES (pH 7.4). CFTR was activated by adding forskolin and 3-isobutyl-1-methylxanthine. The holding potential was −40 mV. For volume-sensitive Cl^- currents, the pipette solution contained 145 mM NMDG-Cl, 5 mM EGTA, 1 mM $MgCl_2$, 3 mM Mg-ATP, and 20 mM HEPES (pH 7.4), and the bath solution contained 126 mM NMDG-Cl, 1 mM $CaCl_2$, 1 mM $MgCl_2$, 10 mM glucose, 10 mM HEPES (pH 7.4), and/or 45 mM sorbitol. For Ca^{2+}-activated Cl^- currents, the pipette solution contained 147 mM NMDG-Cl, 10 mM EGTA, 6.93 mM $CaCl_2$, 1 mM $MgCl_2$, 3 mM Mg-ATP, and 10 mM HEPES (pH 7.4) (free Ca^{2+} concentration 400 nM), and the bath solution contained 148 mM NMDG-Cl, 1 mM $MgCl_2$, 10 mM glucose, and 10 mM HEPES (pH 7.4).

All experiments were performed at room temperature, and the current output was filtered at 5 kHz. Currents were digitized and analyzed using an AxoScope 8.1 system and a Digidata 1322A analog/digital converter (Axon Instruments, Union City, CA). Mean currents were normalized as current

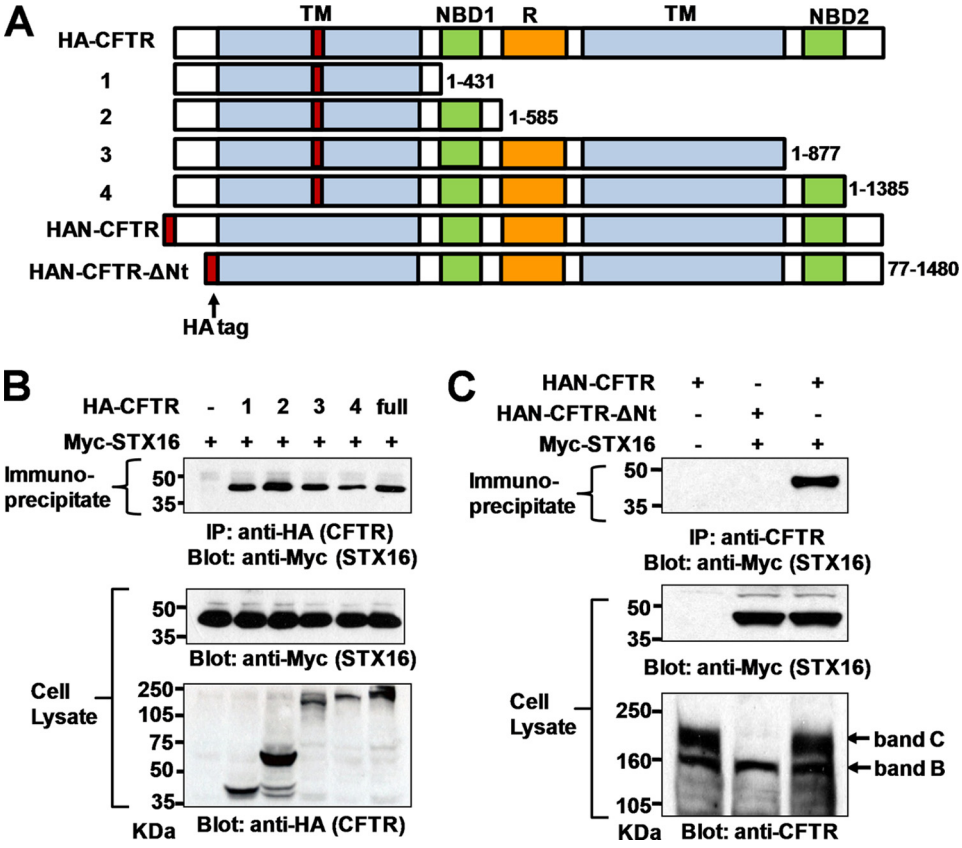

FIGURE 3. **Domain-specific protein-protein interaction between STX16 and CFTR.** *A*, a schematic diagram of CFTR variants used in this study is shown. *B* and *C*, HEK 293 cells were transiently transfected with the HA-tagged CFTR variants and/or Myc-tagged STX16 plasmids. Protein samples were precipitated with anti-CFTR M3A7, and immunoblotting was performed with anti-Myc (STX16). In immunoblotting, 50 and 10 μg of proteins were loaded into each lane for CFTR and STX16, respectively, and immunoprecipitation (*IP*) was performed with a total of 500 μg cell lysate. *band B*, ER core-glycosylated CFTR; *band C*, mature complex-glycosylated CFTR; *full*, full-length; *NBD*, nucleotide binding domain; *TM*, transmembrane domain; *R*, regulatory domain.

currents (Fig. 1, *E* and *F*), indicating that STX16 depletion specifically affects CFTR activity in T84 cells.

Physical Interaction between STX16 and CFTR—To explore underlying mechanisms involved in the STX16-mediated regulation of CFTR, physical interaction between STX16 and CFTR was examined. In T84 cells and rat colon, which endogenously express both STX16 and CFTR proteins, immune-complexes precipitated by the anti-CFTR M3A7 antibody contained STX16, suggesting that native CFTR and STX16 associate in a protein complex (Fig. 2*A*). Next, the relationship between CFTR and STX16 was evaluated by double immunostaining in rat colonic mucosa (Fig. 2*B*). STX16 was highly expressed in the apical and subapical regions of colonic crypt cells, and CFTR was concentrated in the apical area. Consequently, STX16 colocalized with CFTR near the apical regions, where CFTR plays a major role in ion transport and fluid secretion. To further determine the specific subcellular localization of STX16 bound to CFTR, T84 cells were cultured on a permeable support and immunostained. To enhance the visibility of CFTR protein, exogenous CFTR was additionally expressed using transient transfection with pCMV-CFTR. Localizations of CFTR and STX16 in the polarized T84 monolayers were examined using fluorescent images of the vertical *z* axis sections, and fluorescence intensities of CFTR (*green*) and STX16 (*red*) were quantified with MetaMorph software (Fig. 2*C*). Expression of CFTR was highly concentrated at the apical membrane and subapical regions of T84 epithelial cells. STX16 was abundantly expressed at the subapical and central regions of epithelial cells, where recycling endosomes and TGN are localized. Consequently, CFTR and STX16 were highly colocalized at the subapical regions of the polarized T84 monolayers (Fig. 2*C*, *yellow*).

To identify the CFTR domain that interacts with STX16, co-immunoprecipitation was performed in HEK 293 cells using deletion constructs of CFTR (Fig. 3*A*). The co-immunoprecipitation results suggest that the N terminus of CFTR is required for interaction with STX16 (Fig. 3, *B* and *C*). However, the N terminus deletion of CFTR evoked a processing defect and eliminated the mature complex-glycosylated form of CFTR (band *C*) in lysate immunoblot (Fig. 3*C*). It has already been shown that deletion of CFTR N terminus disrupts normal CFTR biosynthesis and maturation in mammalian cells (18, 19). Therefore, to confirm the co-immunoprecipitation result and further characterize the interaction, GST pulldown assays were performed. Cytosolic domains of CFTR and STX16 were GST- and His_6-tagged, respectively (Fig. 4, *A* and *C*). Then, the GST-tagged CFTR domains (GST-CFTR-N-term, GST-CFTR-NBD1, GST-CFTR-NBD2, and GST-CFTR-C-term) were incubated with the His_6-tagged cytosolic domain of STX16 (His_6-STX16-ΔTM), and proteins bound to glutathione beads were blotted with the anti-His antibody. Consistent with the co-immunoprecipitation results, the CFTR N terminus was responsible for interaction with STX16 (Fig. 4*B*). Next, to identify the CFTR interacting domain in STX16, three His_6-tagged truncated STX16 proteins (N terminus (His_6-STX16-N-term), middle helix-containing region (His_6-STX16-Habc), and SNARE domain (His_6-STX16-SNARE)), were incubated with GST-CFTR-N-term, and protein samples were purified with glutathione beads. The pulldown assay showed that middle region of STX16, which contains helices a, b, and c (Habc) (20), binds to the N terminus of CFTR (Fig. 4*D*). Taken together, these data indicate that STX16 directly associates with the CFTR N terminus via its Habc-containing helix domain and is co-localized with CFTR at the apical and subapical regions of colonic epithelial cells.

Molecular Mechanism of CFTR Regulation by STX16—Two possibilities were examined to determine the molecular mech-

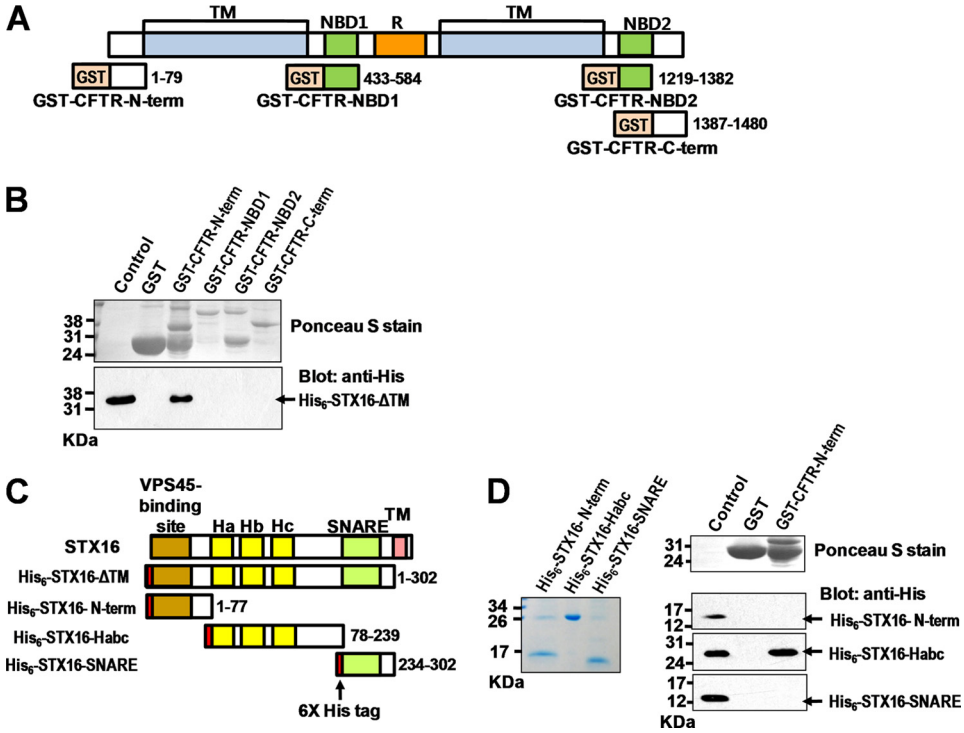

FIGURE 4. ***In vitro* interaction between STX16 and CFTR.** *A*, shown is a schematic diagram of the CFTR cytosolic domains fused with GST that were used for pulldown assays. *B*, expressions of GST-fused CFTR domains are visualized by the Ponceau S stain (*upper panel*). GST pulldown assays were performed using 10 μg of purified recombinant His_6-tagged STX16-ΔTM and 50 μg of each GST-fusion protein (*lower panel*). *C*, shown is a schematic diagram of STX16 domains tagged with His_6. *D*, expressions of His_6-tagged STX16 domains used in pulldown assays are visualized by the Coomassie Brilliant Blue staining (*left panel*). GST pulldown assays were performed using 50 μg of the GST-fused N terminus tail of CFTR (*GST-CFTR-N-term*) and 10 μg of each purified recombinant His_6-tagged STX16 domains (*right panel*). In the control lane in immunoblots, 1 μg of each His_6-tagged protein was loaded. *TM*, transmembrane domain.

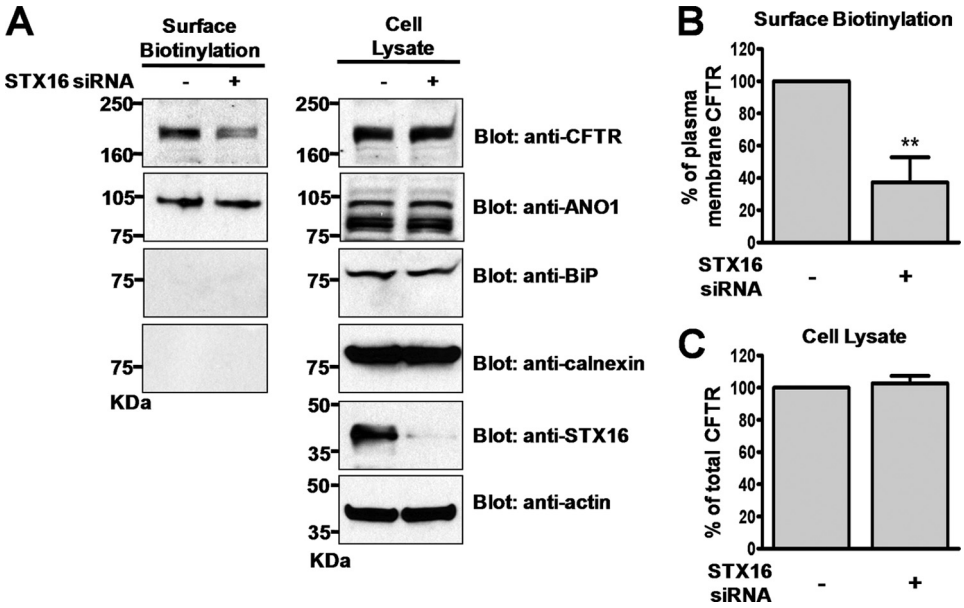

FIGURE 5. **Effect of STX16 depletion on the surface expression of CFTR in T84 cells.** T84 monolayers were transfected with control or STX16-specific siRNA (100 nM). The siRNA transfection method was described under "Experimental Procedures." *A*, surface-biotinylated proteins and whole cell lysates were immunoblotted with anti-CFTR, anti-ANO1, anti-BiP, anti-calnexin, anti-STX16, and anti-β-actin. Cell surface-specific labeling of proteins was confirmed by the absence of ER-localized proteins (calnexin and BiP) in the biotinylated fraction. The amount of surface-biotinylated proteins (*B*) and cell lysates (*C*) was quantified with the Multi Gauge Version 3.0 software package ($n = 3$). **, $p < 0.05$, difference from control.

anism that is responsible for STX16 depletion-induced reduction in the CFTR Cl^- channel activity (Fig. 1*D*). The first possibility is reduced membrane expression of CFTR. SNARE proteins are involved in the sorting, trafficking, and endocytic recycling of cargo proteins (20). Therefore, STX16 may coordinate these processes involved in the CFTR surface expression. Surface biotinylation was performed in T84 cells after transfection with the control scrambled or STX16 siRNAs. As shown in Fig. 5, STX16 silencing reduced CFTR membrane expression by 62.8 ± 6.9% without affecting total amount of CFTR protein in cell lysates. Furthermore STX16 depletion had no significant effect upon the surface expression of the Ca^{2+}-activated chloride channel, Ano1/TMEM16A. This result suggests that STX16 mediates CFTR surface expression by facilitating either the anterograde trafficking of CFTR or the recycling of endocytosed CFTR.

STX16 was shown to be involved in recycling endosome-to-TGN retrograde transport (12) and mediates insulin-stimulated glucose transporter 4 transport to the surface membrane (21). Therefore, the role of STX16 in CFTR recycling was examined using the apical recycling assays of surface-biotinylated protein in polarized T84 monolayers. Cells were stimulated with forskolin after clearing residual surface biotinylated protein with MESNA, because activation of protein kinase A facilitates CFTR trafficking from intracellular compartments to the plasma membrane (22). In T84 cells transfected with control siRNA, 74.6 ± 7.4% of internalized CFTR recycled to the plasma membrane during a10-min forskolin stimulation. However, depletion of STX16 decreased this value to 45.3 ± 7.3% (Fig. 6). Thus, the proper copy number of CFTR channels on the plasma membrane is maintained by STX16-mediated CFTR recycling.

The second potential mechanism by which STX16 depletion inhibits CFTR Cl^- channel activity could be

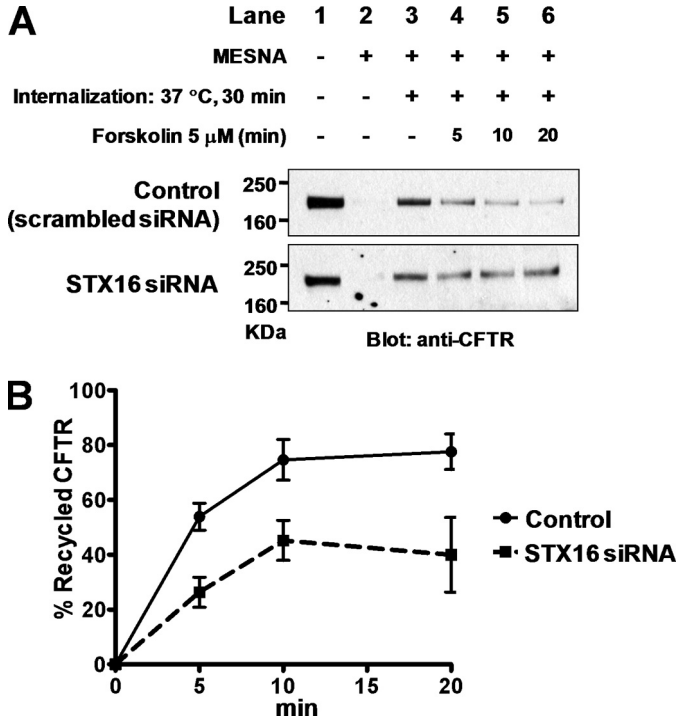

FIGURE 6. **Effect of STX16 depletion on the apical recycling of CFTR in T84 cells.** Apical recycling was assayed in T84 monolayers. The plasma membrane proteins on apical side were biotinylated and then internalized for 30 min at 37 °C. Proteins remaining at the cell surface were stripped of biotin with the sodium 2-mercaptoethanesulfonate stripping buffer. Recycling of internalized, biotinylated CFTR was stimulated with 5 μM forskolin for 5, 10, or 20 min. Non-recycled, biotinylated proteins were collected and immunoblotted. *A*, representative CFTR immunoblot of apical recycling assays in T84 monolayers transfected with scrambled or STX16-specific siRNA is shown. *Lane 1*, total apical membrane CFTR; *lane 2*, sodium 2-mercaptoethanesulfonate (*MESNA*) stripping control; *lane 3*, internalized CFTR after 30 min at 37 °C; *lanes 4*, *5*, and *6*, internalized CFTR that remained in the cells after 5, 10, and 20 min forskolin stimulation (5 μM). The difference between *lanes 3* and *lanes 4*, *5*, and *6* represents recycled CFTR. *B*, shown is quantitative analysis of apical CFTR recycling in T84 cells transfected with control or STX16 siRNA ($n = 4$).

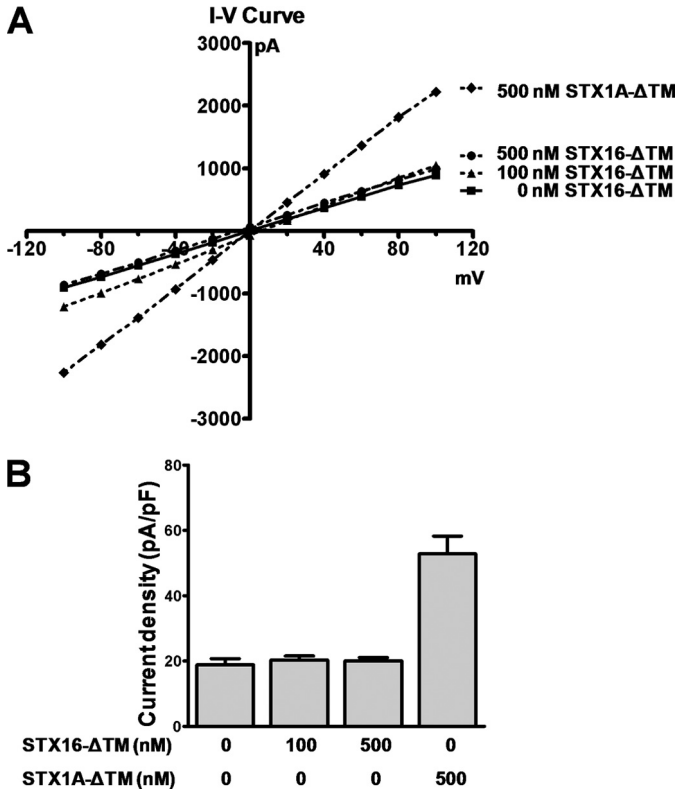

FIGURE 7. **Effect of STX16 cytosolic domain on the CFTR channel activity.** Whole cell Cl^-currents were measured with patch pipettes containing the purified recombinant cytosolic domain of STX16 (His_6-STX16-ΔTM). The cytosolic domain of STX1A (His_6-STX1A-ΔTM) was used as a positive control. *A*, cAMP-activated Cl^- channel activity was determined in T84 cells using patch pipettes containing 0, 100, 500 nM His_6-STX16-ΔTM or 500 nM of His_6-STX1A-ΔTM. Cells were stimulated with forskolin (5 μM), and currents were measured after a 10-min equilibration with pipette solution that contained recombinant proteins. The current-voltage (*I-V*) relationships were obtained with a step pulse from −100 to + 100 mV applied at peak current. *B*, mean currents measured at −40 mV holding potential were normalized as current densities (pA/pF; 0 nM STX16-ΔTM, $n = 7$; 100 nM STX16-ΔTM, $n = 11$; 500 nM STX16-ΔTM, $n = 7$; 500 nM STX1A- ΔTM, $n = 6$).

due to a direct effect of STX16 on CFTR channel function. STX1A was previously shown to modulate CFTR-mediated Cl^- current via a direct protein-protein interaction with the CFTR N terminus (7, 18). To investigate this possibility, we performed whole-cell patch clamp in T84 cells using a patch pipette containing recombinant STX16 lacking the transmembrane domain (STX16-ΔTM) (Fig. 7). In control experiments, inclusion of the cytosolic domain of STX1A (STX1A-ΔTM) in the patch pipette solution resulted in a 2–3-fold increase of CFTR currents within 10 min of membrane rupture by patch pipette (Fig. 7) as previously described (7). Treatment with STX1A-ΔTM augments CFTR currents by disrupting interactions with endogenous membrane-anchored STX1A that normally attenuates the activity of native CFTR in T84 cells (7). However, inclusion of the cytosolic domain of STX16 (STX16-ΔTM) in the patch pipette produced no acute effects on the CFTR chloride current in T84 cells (Fig. 7). Taken together, the above results suggest that STX16 regulates CFTR activity by increasing surface abundance via its membrane trafficking SNARE function rather than directly affecting CFTR channel.

DISCUSSION

The present study provides direct evidence that STX16 is a part of the CFTR trafficking machinery and regulates its surface expression in polarized epithelial cells. Several lines of evidence support a role of STX16 in CFTR trafficking and surface expression. First, the CFTR N terminus mediates its direct interaction with STX16 (Figs. 2–4). The N terminus of CFTR seems to play an important role for its intracellular trafficking and processing. Among syntaxins, STX1A and endosomal SNAREs, including STX7 and STX8, are known to bind to the CFTR N terminus (18, 23). Filamins, which are actin-binding proteins that stabilize CFTR at the cell surface, and the cysteine string protein, which is a chaperone that modulates CFTR maturation, also bind to the N terminus of CFTR (19, 24). In addition, the N terminus contains an internalization signal that appears to be important for CFTR endocytosis by an unknown mechanism (25).

Second, STX16 depletion decreases CFTR surface expression (Figs. 5 and 6). It has been reported that Tlg2p, the yeast homologue of mammalian STX16, is localized to the TGN and early endosomes and up-regulates the membrane trafficking of proteins such as casein kinases (26, 27). The glucose transporter

glucose transporter 4 recycles to the cell surface via a STX16-dependent mechanism (6, 21). In accordance with previously identified functions of STX16, we demonstrate here that STX16 facilitates surface expression of CFTR on the apical membrane of epithelial cells. The fact that STX16 is linked to early/recycling endosome-to-TGN retrograde transport indicates that it may be involved in the surface recycling of CFTR via TGN (Fig. 7). Several Rab GTPases, which regulate endosome-to-TGN transport, have been shown to affect CFTR intracellular trafficking. Rab11 controls early endosome-to-TGN trafficking of CFTR and its recycling by an Rme1-dependent vesicular transport mechanism (3, 28). In addition, Rab9 mediates CFTR membrane transport via the late endosome-to-TGN pathway (3). The precise role of STX16 in CFTR trafficking as well as the cognate SNARE partners involved requires further investigation.

SNAREs play an important role in intracellular trafficking of ion channels and transporters. As members of the (t)-SNARE protein family, several syntaxins have been suggested to be involved in the intracellular trafficking and regulation of CFTR. As mentioned earlier, STX1A has been shown to regulate CFTR channel activity directly through a protein-protein interaction (7, 18, 29). In addition, it has been reported that overexpression of STX5, which is required for the fusion of coat protein complex II (COPII) transport vesicles with acceptor Golgi membranes, inhibits CFTR processing in some cell lines and that overexpression of STX13, which resides in early and late recycling endosomes, blocks CFTR maturation in baby hamster kidney cells (4). However, CFTR trafficking in heterologous expression systems does not exactly reflect that in polarized epithelial cells (14, 30).

We have initially studied the effects of STX16 on CFTR trafficking in non-polarized HEK 293 cells. Overexpression of STX16 increased the surface expression and current density of CFTR (supplemental Fig. 2). Interpretation of these results should be done carefully and with appropriate reservations, because the consequences of STX overexpression could be complex and unpredictable. Overexpression of STXs may reinforce the action of these proteins or may actually inhibit their action by disrupting the stoichiometric balance in relation to other SNARE proteins (23). For example, overexpression of wild type STX6 was shown to increase tumor necrosis factor-α (TNFα) surface delivery and secretion, whereas overexpression of a dominant negative cytoplasmic STX6 reduced TNFα delivery (31). Contrastingly, overexpression resulted in loss-of-function for certain STXs, including STX5, which hindered the ER-to-Golgi transport of vesicular stomatitis virus G protein (4), and STX7 and STX8, which inhibited the apical targeting of CFTR (23). In addition, the effect of STX overexpression depends on the cell types concerned. Overexpression of STX5 inhibited the ER-to-Golgi transport of CFTR in HEK 293T and HeLa cells but not in baby hamster kidney cells (4). In the case of STX16, its overexpression in HEK 293 cells showed gain-of-function effects on CFTR expression and function (supplemental Fig. 2), which are comparable with those observed in T84 cells (Figs. 1 and 5).

Another important group of proteins that is involved in the regulation of CFTR expression and activity is PDZ (PSD-95/discs large/ZO-1)-based adaptor proteins including NHERFs and Shank2 (15, 32). Both NHERFs and Shank2 increase surface expression of CFTR, although they exert opposite effects on cAMP-induced activation of CFTR Cl^- channel activity (11, 33). Interestingly, some PDZ proteins, such as FIG/CAL and syntenin-1, have been shown to associate with STXs and participate in the intracellular trafficking of CFTR and other membrane proteins (34–36). Therefore, it will also be an interesting subject to investigate whether PDZ-based adaptors are involved in the effects of STX16 on CFTR trafficking.

Considering its rapid internalization and relatively low translation rate, the recycling of endocytosed CFTR is essential to maintain the proper number of functional CFTR at the cell surface (37). The maintenance of steady-state cell surface level of CFTR is primarily due to recycling of internalized CFTR rather than insertion of newly synthesized CFTR (28). The ΔF508-CFTR mutant has a folding defect and is mostly degraded by the ER-associated degradation pathway. Some maneuvers, such as low temperature incubation, and small molecules called correctors can partially correct processing defects of ΔF508-CFTR and facilitate its delivery to the surface membrane. However, ΔF508-CFTR exhibits a markedly reduced cell surface stability compared with wild type CFTR (3, 38). Studies have demonstrated an almost 10-fold decrease in the surface half-life of ΔF508-CFTR (39). Interestingly, overexpression of STX16 increased the membrane expression of ΔF508-CFTR that was rescued by the low temperature incubation (27 °C), whereas depletion of STX16 by siRNA showed the opposite effect in HEK 293 cells (supplemental Fig. 3). These results imply that the reduced surface half-life of ΔF508-CFTR can be overcome at least partially by increasing the efficiency of recycling.

In summary, our results indicate that STX16 actively participates in the trafficking and recycling of CFTR. Understanding the mechanism by which STX16 modulates CFTR activity will contribute to develop therapeutic strategies to treat CF that is caused by aberrant intracellular trafficking of membrane proteins.

Acknowledgments—We thank Hyun Woo Park and Seo Yeon Kyung for editorial assistance, and we also wish to thank the Yonsei-Carl Zeiss, Advanced Imaging Center, Yonsei University College of Medicine, for technical assistance.

REFERENCES

1. Amaral, M. D. (2004) *J. Mol. Neurosci.* **23,** 41–48
2. Quinton, P. M. (1999) *Physiol. Rev.* **79,** S3–S22
3. Gentzsch, M., Chang, X. B., Cui, L., Wu, Y., Ozols, V. V., Choudhury, A., Pagano, R. E., and Riordan, J. R. (2004) *Mol. Biol. Cell* **15,** 2684–2696
4. Yoo, J. S., Moyer, B. D., Bannykh, S., Yoo, H. M., Riordan, J. R., and Balch, W. E. (2002) *J. Biol. Chem.* **277,** 11401–11409
5. Teng, F. Y., Wang, Y., and Tang, B. L. (2001) *Genome Biol.* **2,** REVIEWS3012
6. Saxena, S., Quick, M. W., Tousson, A., Oh, Y., and Warnock, D. G. (1999) *J. Biol. Chem.* **274,** 20812–20817
7. Naren, A. P., Nelson, D. J., Xie, W., Jovov, B., Pevsner, J., Bennett, M. K., Benos, D. J., Quick, M. W., and Kirk, K. L. (1997) *Nature* **390,** 302–305
8. Mallard, F., Tang, B. L., Galli, T., Tenza, D., Saint-Pol, A., Yue, X., Antony, C., Hong, W., Goud, B., and Johannes, L. (2002) *J. Cell Biol.* **156,** 653–664

9. Tang, B. L., Low, D. Y., Lee, S. S., Tan, A. E., and Hong, W. (1998) *Biochem. Biophys. Res. Commun.* **242,** 673–679
10. Han, W., Kim, K. H., Jo, M. J., Lee, J. H., Yang, J., Doctor, R. B., Moe, O. W., Lee, J., Kim, E., and Lee, M. G. (2006) *J. Biol. Chem.* **281,** 1461–1469
11. Kim, J. Y., Han, W., Namkung, W., Lee, J. H., Kim, K. H., Shin, H., Kim, E., and Lee, M. G. (2004) *J. Biol. Chem.* **279,** 10389–10396
12. Chua, C. E., and Tang, B. L. (2008) *Mol. Membr. Biol.* **25,** 35–45
13. Piper, R. C., Hess, L. J., and James, D. E. (1991) *Am. J. Physiol.* **260,** C570–C580
14. Silvis, M. R., Bertrand, C. A., Ameen, N., Golin-Bisello, F., Butterworth, M. B., Frizzell, R. A., and Bradbury, N. A. (2009) *Mol. Biol. Cell* **20,** 2337–2350
15. Lee, J. H., Richter, W., Namkung, W., Kim, K. H., Kim, E., Conti, M., and Lee, M. G. (2007) *J. Biol. Chem.* **282,** 10414–10422
16. Namkung, W., Kim, K. H., and Lee, M. G. (2005) *Gastroenterology* **129,** 1979–1990
17. Dulubova, I., Yamaguchi, T., Gao, Y., Min, S. W., Huryeva, I., Südhof, T. C., and Rizo, J. (2002) *EMBO J.* **21,** 3620–3631
18. Naren, A. P., Quick, M. W., Collawn, J. F., Nelson, D. J., and Kirk, K. L. (1998) *Proc. Natl. Acad. Sci. U.S.A.* **95,** 10972–10977
19. Thelin, W. R., Chen, Y., Gentzsch, M., Kreda, S. M., Sallee, J. L., Scarlett, C. O., Borchers, C. H., Jacobson, K., Stutts, M. J., and Milgram, S. L. (2007) *J. Clin. Invest.* **117,** 364–374
20. Hong, W. (2005) *Biochim. Biophys. Acta* **1744,** 493–517
21. Proctor, K. M., Miller, S. C., Bryant, N. J., and Gould, G. W. (2006) *Biochem. Biophys. Res. Commun.* **347,** 433–438
22. Guggino, W. B., and Stanton, B. A. (2006) *Nat. Rev. Mol. Cell Biol.* **7,** 426–436
23. Bilan, F., Nacfer, M., Fresquet, F., Norez, C., Melin, P., Martin-Berge, A., Costa de Beauregard, M. A., Becq, F., Kitzis, A., and Thoreau, V. (2008) *Exp. Cell Res.* **314,** 2199–2211
24. Zhang, H., Peters, K. W., Sun, F., Marino, C. R., Lang, J., Burgoyne, R. D., and Frizzell, R. A. (2002) *J. Biol. Chem.* **277,** 28948–28958
25. Prince, L. S., Peter, K., Hatton, S. R., Zaliauskiene, L., Cotlin, L. F., Clancy, J. P., Marchase, R. B., and Collawn, J. F. (1999) *J. Biol. Chem.* **274,** 3602–3609
26. Abeliovich, H., Grote, E., Novick, P., and Ferro-Novick, S. (1998) *J. Biol. Chem.* **273,** 11719–11727
27. Panek, H. R., Conibear, E., Bryan, J. D., Colvin, R. T., Goshorn, C. D., and Robinson, L. C. (2000) *J. Cell Sci.* **113,** 4545–4555
28. Picciano, J. A., Ameen, N., Grant, B. D., and Bradbury, N. A. (2003) *Am. J. Physiol. Cell Physiol.* **285,** C1009–C1018
29. Chang, S. Y., Di, A., Naren, A. P., Palfrey, H. C., Kirk, K. L., and Nelson, D. J. (2002) *J. Cell Sci.* **115,** 783–791
30. Ameen, N., Silvis, M., and Bradbury, N. A. (2007) *J. Cyst. Fibros.* **6,** 1–14
31. Murray, R. Z., Wylie, F. G., Khromykh, T., Hume, D. A., and Stow, J. L. (2005) *J. Biol. Chem.* **280,** 10478–10483
32. Singh, A. K., Riederer, B., Krabbenhöft, A., Rausch, B., Bonhagen, J., Lehmann, U., de Jonge, H. R., Donowitz, M., Yun, C., Weinman, E. J., Kocher, O., Hogema, B. M., and Seidler, U. (2009) *J. Clin. Invest.* **119,** 540–550
33. Short, D. B., Trotter, K. W., Reczek, D., Kreda, S. M., Bretscher, A., Boucher, R. C., Stutts, M. J., and Milgram, S. L. (1998) *J. Biol. Chem.* **273,** 19797–19801
34. Charest, A., Lane, K., McMahon, K., and Housman, D. E. (2001) *J. Biol. Chem.* **276,** 29456–29465
35. Cheng, J., Cebotaru, V., Cebotaru, L., and Guggino, W. B. (2010) *Mol. Biol. Cell* **21,** 1178–1187
36. Ohno, K., Koroll, M., El Far, O., Scholze, P., Gomeza, J., and Betz, H. (2004) *Mol. Cell. Neurosci.* **26,** 518–529
37. Okiyoneda, T., and Lukacs, G. L. (2007) *Biochim. Biophys. Acta* **1773,** 476–479
38. Heda, G. D., Tanwani, M., and Marino, C. R. (2001) *Am. J. Physiol. Cell Physiol.* **280,** C166–C174
39. Sharma, M., Pampinella, F., Nemes, C., Benharouga, M., So, J., Du, K., Bache, K. G., Papsin, B., Zerangue, N., Stenmark, H., and Lukacs, G. L. (2004) *J. Cell Biol.* **164,** 923–933